HONGRUI ZHANG
DENGHONG WANG
SHENGQING XIONG
and
ZHENGGUO FAN

Compiling methods of large-area aeromagnetic map based on multiple data sources

With the compilation of the 1:1,000,000 Chinese land area aeromagnetic map as an example

In this paper, the author has conducted a research on the compiling methods and technologies of large-area aeromagnetic maps with aeromagnetic data collected in different times, according to different scales, at different flying altitudes, with different surveying instruments, and of different qualities and precision. The focus of this research is on the standardized processing technique of data in independent survey areas, the splicing methods and splicing principles of grids, and the high-precision control framework grid technology which retains the magnetic field information of lithosphere. With the 1:1,000,000 Chinese land area aeromagnetic map as an example, the author has conducted a positive probe into the mapping methods and mapping effects.

Keywords: multiple data source, grid data, standardization, aeromagnetic mapping, high precision control framework grid.

I. Introduction

The large-area aeromagnetic map is a basic picture material for studying regional geotectonics, geological background and the law of mineralization. It's an important basic source for evaluating regional mine resource potential and is also very valuable for other basic geological studies. Therefore, research on the compilation of maps of this kind has both strategic and pragmatic significance.

The aerospace and marine magnetic field survey work has been going on for over half a century and magnetic data that almost covers the entire globe has been collected. The National Geophysical Data Center (S. Maus and T. Sazonova, 2007) launched the World Digital Magnetic Anomaly Map project and 23 regions and countries have joined the project (Chiappini, 2000; Socias, 1996; Socias, 1991; Vine, 1963). To smoothly splice the global magnetic fields, theoretical studies including long wavelength filtering (Cordell L.1985), shortwave data splicing and applying CHAMP satellite magnetic field to simulate lithosphere magnetic field have been conducted in advance, laying a solid theoretical foundation for large-area aeromagnetic mapping (Fairhead, 1997; Maus, 2007, 2002).

To support the compilation of the 1:1,000,000 Chinese land area aeromagnetic map, on the basis of the compiling methods of WDMAM, the author has analyzed technical problems including the huge gaps between individual surveying areas in terms of precision and quality, the accumulation of horizontal deviations of long wavelength in grid splicing and the loss of background magnetic field features of lithosphere.

In response to the technical problems above, after finishing the preparatory work including original data optimization of independent survey areas and grid data pre-processing, and with the aeromagnetic surveying data collected over the past 50 years and more in China, the author has conducted a research on the grid splicing technology (WANG Naidong, 2007; WEN Zhenhe, 2011), proposed to solve the problems of the accumulation of long wavelength horizontal deviation in the traditional mapping methods by using the large-area high-precision control grid building technology, and compiled a new aeromagnetic map of the Chinese land area.

2. Study of the multiple data source standardization methods

2.1 Analysis on the differences in the surveying precision of multiple source data

Since the 1950s, China has measured and interpreted over 560 aeromagnetic surveying areas of various scales (1:1,000,000 – 1:5,000). The total length is 17.194 million km and the total area surveyed is 22.336 million km^2, basically covering the entire land area of China. The surveying work in these independent survey areas have been conducted by over 20 aerospace and geophysical prospecting institutions, which all differ greatly from each other in terms of surveying equipment, equipment sensitivity, navigation and positioning methods, and ways of data collection (WANG Naidong, 2007). Based on the differences in the navigation and positioning

Messrs. Hongrui Zhang, Institute of Mineral Resources, Chinese Academy of Geophysical Sciences and also CITIC Construction Co. Ltd., Beijing and Denghong Wang, Institute of Mineral Resources, Chinese Academy of Geological Sciences, Beijing 100037 and Shengqing Xiong and Zhengguo Fan, China Aero Geophysical Survey and Remote Sensing Centre for Land and Resources, Beijing 1900083, China. Corresponding author: Email: imr_wanghd@163.com

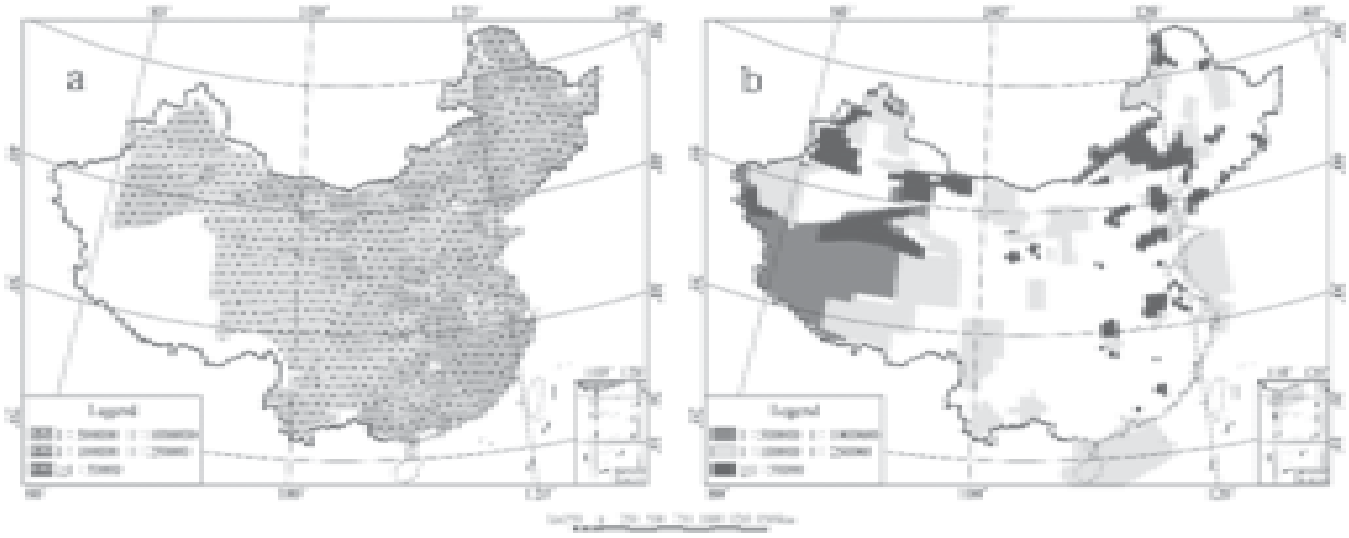

Fig.1 Distribution map of the survey areas where the data used in the aeromagnetic mapping of the Chinese land area is obtained.
(a) distribution map of survey areas where low and medium precision data is obtained;
(b) distribution map of survey areas where low and medium precision data is obtained

TABLE 1 AVERAGE FLYING ALTITUDES OF THE HIGH-PRECISION AEROMAGNETIC SURVEY AREAS

Scale (10,000)	Flying altituded ≤1 50m surveyed area (km^2)	Flying altitude 150-300m surveyed area (km^2)	Flying altitude 300- 500m surveyed area (km^2)	Flying altitude >500m surveyed area (km^2)
>=1:5	407270	275063	51694	414560
1:10-1:25	1009931	1500525	169374	658836
1:50-1:100	16930	0	0	1150323
Total	1434130	1775588	221068	2223719
Percentage	25.4%	31.4%	3.9%	39.3%

methods, ways of data recording and survey precision, the development roughly consists of the following 3 phases:

(1) Low precision phase (1950s – early 1970s). The survey in this phase mainly relied on airborne fluxgate magnetometers, visual navigation, direction indicator positioning, and simulated recording. The survey precision was below ±10nT, the positioning precision was generally about 700 meters and the altitude data was lacking. (2) Medium precision survey phase (middle 1970s – late 1980s). The survey in this phase mainly relied on proton-precision magnetometers and partly relied on optical-pump magnetometers. It combined both Doppler radar navigators and radio instruments for positioning. The recording was mainly simulated and partly digital. The survey precision was ±5 -10nT, the positioning precision was generally below 100 meters and the altitude data was lacking. (3) High precision survey phase (early 1990s – now). The measure in this phase mainly relies on optical-pump magnetometers, GPS navigation, and digital recording. The survey precision is below ±3nT, the positioning precision is below 10 meters and there's altitude data collected via radar in every survey spot.

Considering the quality of the aeromagnetic data collected in China as indicated above, the author has selected 425 survey areas of low and medium precision (Fig.1a) for preferential use in the mapping, whose survey workload was 11.538 million km and surveyed area was 16.682 million km^2. The number of high precision aeromagnetic surveying areas selected for preferential use is 143 (Fig.1b), and the survey workload was 56.56 million km and the surveyed area was 56.54 km^2.

Due to the huge variations in territorial altitudes in China, there're differences at different levels in the flying platforms, survey scales and flying altitudes of the magnetometers. For example, in Fig.1 and Table 1, among the high precision aeromagnetic surveys with altitude records, the areas surveyed at an average flying altitude ≤150m account for 25.4% of the total flying areas, the areas surveyed at an average flying altitude 150m-300m account for 31.4% of the total flying areas, the areas surveyed at an average flying altitude 300m-500m account for 3.9% of the total flying area, and the areas surveyed at an average flying altitude >500m account for 39.3% of the total flying area. The areas surveyed

at an average flying altitude >500m are mainly in the medium and high altitude mountainous areas in the west and southwest of China.

Considering the characteristics of the data from multiple sources, the general principle of selecting the data is: preferentially use the data of high precision and high quality; for areas where high quality data is not available, successively use the data of comparatively better quality; and ensure that new data cover old data, data of big scale cover data of small scale and low flying altitude data cover high altitude data.

2.2 Study of the standardization method of source data

Given that data collected in different times, of different precision, in different scales and at different flying altitudes must be spliced together into a single one data grid, there's a high requirement for the standardization level of the source data in independent survey areas. In this paper, we have conducted five standardization operations for the data in independent survey areas, i.e., international geomagnetic reference field correction, tie line leveling, noise micro-leveling, standardized gridding and altitude reference surface reduction.

2.2.1 International geomagnetic reference field correction (IGRF correction)

As the Earth magnetic field intensity varies along the altitude and the latitude, we must correct the altitude and adjust the field during the high-precision mapping process. Currently, the international norm is to use the IGRF calculated with the Gauss spherical harmonic analysis method as the normal Earth magnetic field. The IGRF model coefficient is adjusted every five years and the reference field times is marked. The IGRF correction is the calculation result of the actual field minus IGRF.

Because this aeromagnetic mapping deals with survey data collected in different times over the past 50 years and more, all the magnetic fields in every independent survey area must be corrected (Backus, 1970) according to the corresponding IGRF model of their time (GAO Guoming, 2010, KANG Guofa, 2009, 2010).

2.2.2 Tie line leveling

In the surveying process, due to the variations in flying altitudes, the background fields of the survey line are not on the same level, causing the overall heights of the magnetic intensity of different survey lines to be inconsistent. Such inconsistency has brought a big impact to the picture quality on the map. Horizontal deviations of this kind can be eliminated through the on-the-spot-survey tie line leveling, which may universalize all the survey line background field values in the survey area to the same level.

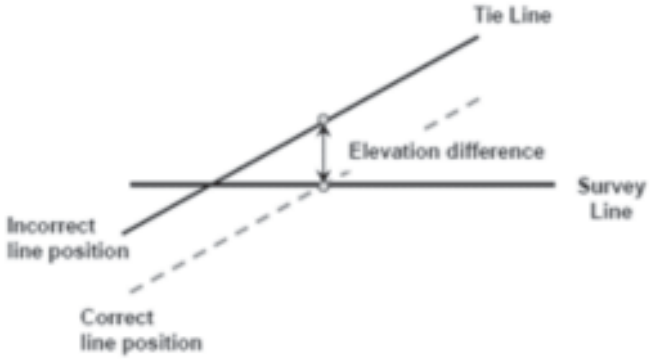

Fig.2 Juncture of the survey line and tie line (from the Geosoft website)

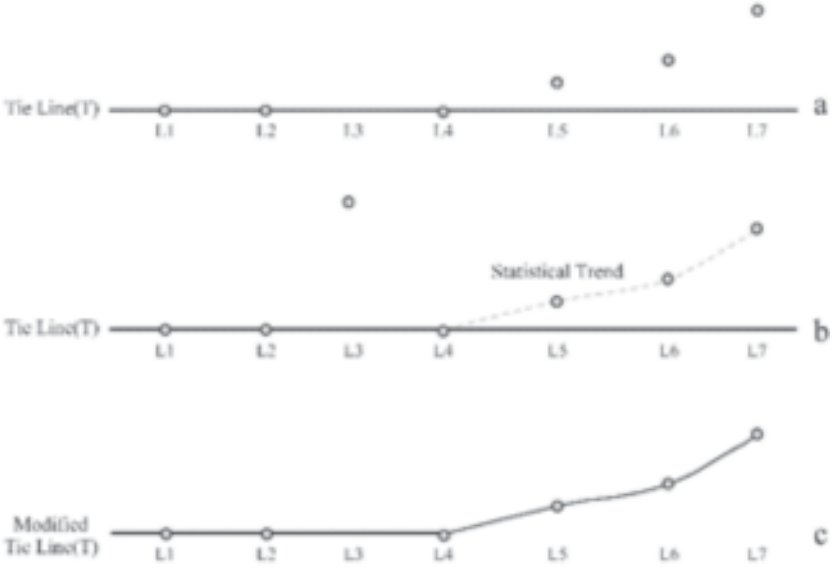

Fig.3 Tie line leveling method (from the Geosoft website)

The principle is to calculate the difference in the magnetic field values (Fig.3a) of the juncture (Fig.2) of the survey line and the tie line one by one. If the magnetic field values of the tie line at the juncture are generally higher or lower than the magnetic field values of the survey line, then their differences might be deemed as being caused by the zero line drift of the tie line. A low-order polynomial curve is fitted with the juncture difference values (Fig.3b), which is equivalent to a low pass filter. After adding the numerical values on the fitted curve to the tie line, a corrected tie line is obtained (Fig.3c)

Then, by subtracting the fitting curve value from the juncture difference value, the remnant difference of the juncture difference value is obtained, which in fact is the high pass component of the low pass filter above. Finally, the remnant difference of the juncture different value is assigned to the survey line and then subtracted from the survey line. In this way, the juncture difference value is respectively shared by the survey line and the tie line – one part is added to the tie line and the other part is subtracted from the survey line. This, in effect, has played the role of eliminating zero line drift of the two survey lines.

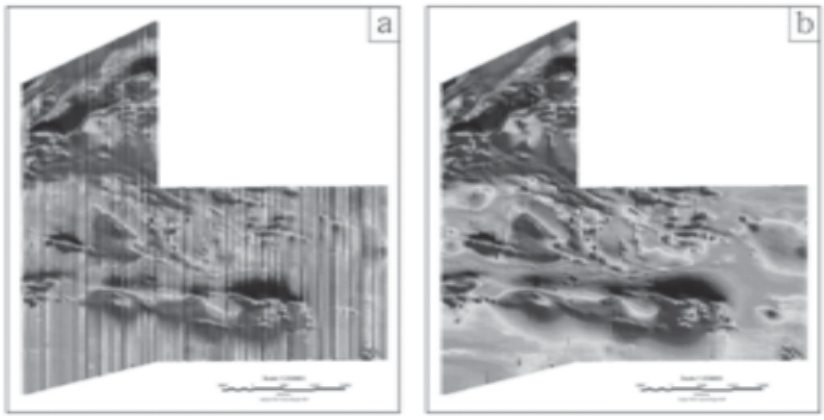

Fig.4 Comparison diagram of the effect before and after tie line leveling. (a) original aeromagnetic shadow image; (b) aeromagnetic shadow image after tie line leveling

Fig.4 offers a comparison between the map effects before and after tie line leveling during an on-the-spot survey. From the figures, it can be seen that through tie line leveling, the stripe-like anomaly of the magnetic field caused by inconsistent background fields can be effectively eliminated.

2.3 Micro-leveling

The tie line leveling eliminates the salient horizontal deviations in the magnetic fields, but a small amount of zero line drift still remains (Minty BRS, 1991). This is caused by the micro variations in flying altitudes and incorrect positioning. This situation is especially severe in areas where the magnetic field gradient variations are intense. If the gap between the tie lines are big and the zero line level of the survey line in between the gap is not even, an empirical method to eliminated these remnant deviations must be adopted, i.e., filtering the level difference between neighboring lines.

The first step in micro-leveling is to grid the survey line data with the minimum curvature method at the optimal spacing and adjust the filter to the Decorrugation frequency domain to filter the waves of the grid data. This filter consists of a 6-order high pass Butterworth filter whose cut-off frequency has been defined and a Cosine Roll filter (Minty, 1991). This filter can create a noise network along the direction of the survey line. The noise network data is extracted and then used to establish a new piece of profile data (noise information). After this is done, the noise network is examined to ensure that this noise is irrelevant between the survey lines.

The second step of micro-leveling is to analyze the noise data profile and confirm the coefficient needed to separate the high frequency geophysical information from the real remnant noise of the survey line. The narrow peaks in the noise profile are deemed as geological information and are retained. In contrast, the low amplitude long wave components are deemed as the real noise and are filtered with the Naudy low pass filter and the Naudy non-linear filter (NaudyH, 1968).

The micro-leveling method described above is widely used in the processing of remote sensing images. Put in a simple way, it is to separate the basic map face information and disturbance information without changing regularities from the data, and then separate information we find useful from the disturbance information and return the useful information to the basic map face information so as to ensure that useful information is not lost (Minty, 1991).

The advantage of micro-leveling is that it completely retains the resolution of the original profile data while not moving or twisting significant geological anomaly (Fig.5).

2.4 Gridding

The gridding of the data in each survey area is conducted via the minimum curvature method (Briggs, 1974, Ash Johnson, 2000), i.e., using the optimal resolution at 1/4 line spacing to grid and universalizing relevant parts to the final mapping grid spacing in the splicing process.

The Minimum Curvature gridding method adopts a minimum curvature profile fitted data point and is a method that can fit the actual data into the most smooth data profile (PGW, 1999), which well conforms to the spatial distribution law of the magnetic field.

It's worth noting that most of the surveyed areas involved in this aeromagnetic mapping provide 1:50,000 high precision data and part of the areas provide data at small scales such as 1:1,000,000 or 1:500,000. Therefore, to prevent magnetic field anomaly or avoid blank grid space, the grid spacing of certain small scale data is reduced gradually (Fig.6) so as to achieve the universalized grid data of 1000m×1000m of the entire country.

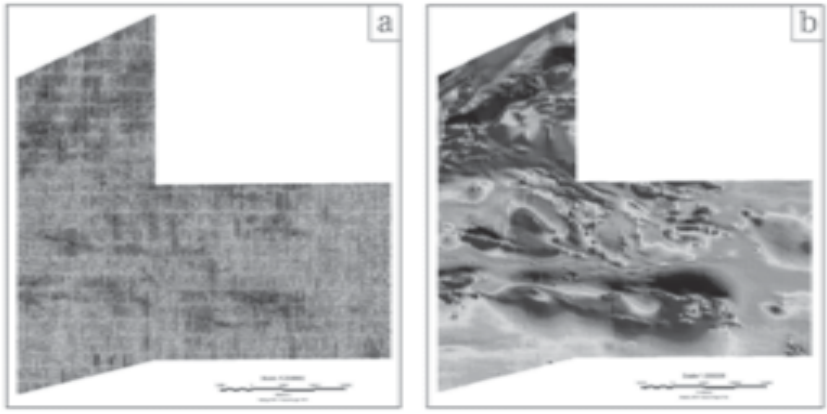

Fig.5 Aeromagnetic micro-leveling effect drawing. (a) 3-D shadow image of the noise network (b) 3-D shadow image after micro-leveling

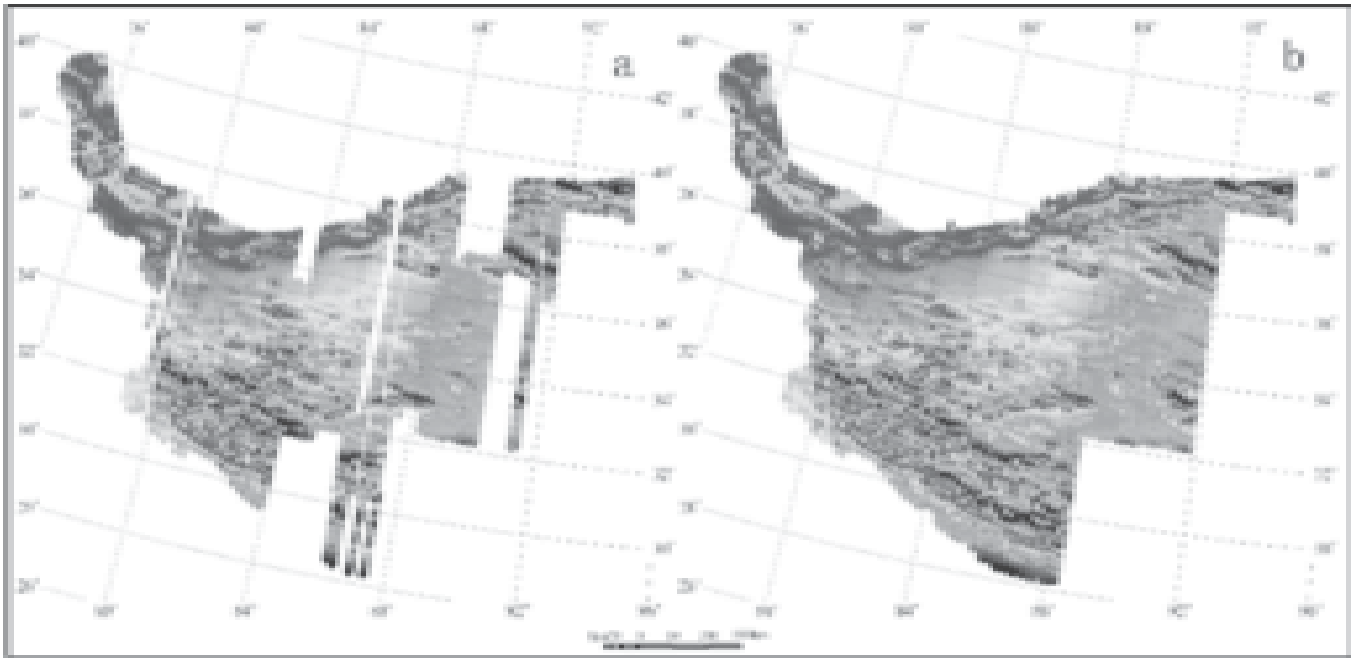

Fig.6 Comparison diagram of grid data from magnetic fields of different grid spacing on the Tibetan Plateau. (a) gridding result of 1-km spacing grids; (a) gridding result of gradually reducing spacing grids

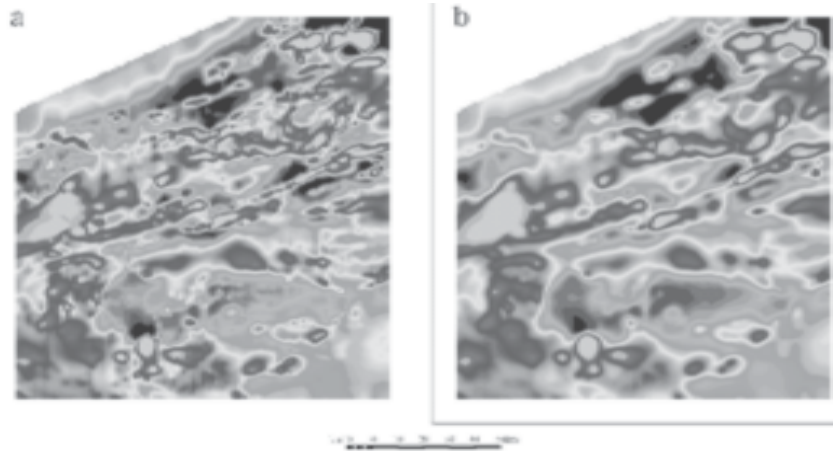

Fig.7 Reference surface reduction result of the high precision aeromagnetic data of a survey area. (a) original data; (b) result after upward continuation to 1000 m

2.5 Reference surface reduction

The flying altitudes of aeromagnetic surveying in the east of China are mostly below 500 meters while those in the western mountainous areas of China are mostly between 500 meters and 1000 meters and a small portion of the areas there are above 1000 meters. From Fig.1b, it can be seen that the high-precision aeromagnetic surveying data are mostly in the middle and west of China and the areas surveyed at a flying altitude above 500 meters account for 39.3% of the total. Therefore, in this mapping, we reduce the reference surface to 1000 meters above the ground.

In order to reduce the data of every independent surveyed area to the same reference surface, for aeromagnetic surveying data with altitude data, the potential field transformation technology is adopted to transfer the aeromagnetic data that deviates from the reference surface to reference surface. For aeromagnetic surveyed data lacking altitude data, the upward continuation method is adopted to reduce the data to the reference surface (Fig.7). If the flying altitude is above the universalized mapping reference surface, no downward continuation will be conducted. Instead, only the magnetic level will be adjusted according to aeromagnetic surveying data of the surrounding high precision control framework so as to achieve the smooth transition of the grid.

3. Analysis of the splicing method of grid data in independent survey areas

Grid data splicing in independent survey areas is the basic method in large-area aeromagnetic mapping. The differences in survey coefficient, noise level, data quality, and sample collection density and the uncertainties in the data splicing boundaries of independent survey areas are key factors that affect grid splicing effects and qualities. The mainstream grid data splicing methods include the blending method and the suture method (Minty, 2003; Paterson N, 1990).

Blending Method: With this method, one piece of grid data may be smoothly transferred to another piece of grid data in the overlapping zone. To be specific, for any point in the overlapping zone, calculate the distances between this point and the two grid boundaries, then use a cosine function to confirm the weight coefficient of the two grid numeric

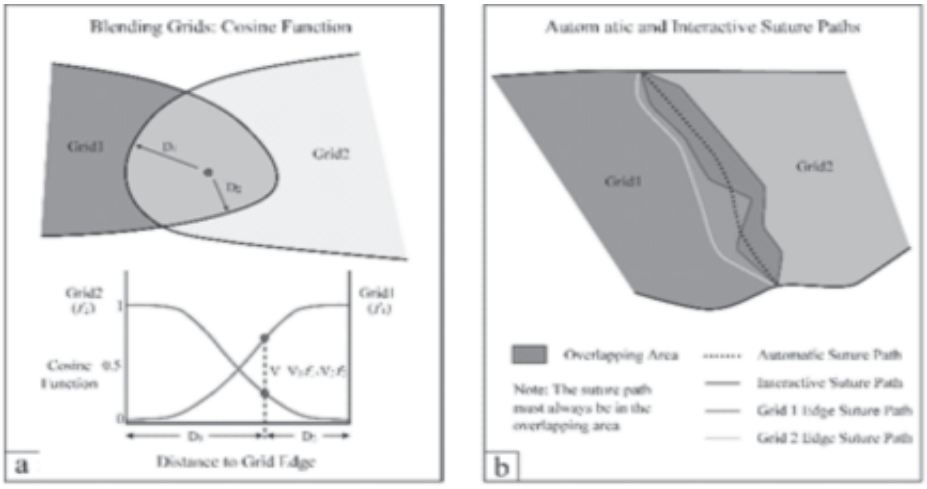

Fig.8 Schematic diagram of the grid splicing methods. (a) schematic diagram of the blending method; (b) schematic diagram of the suture method

values in the calculation (Fig.8a). Finally, respectively multiply the two original grid numeric values with the weight coefficient, add the multiplied result, and the numeric value of the new grid at this point is obtained. The blending method is often used in situation where the magnetic field is relatively still and the transitional trend is obvious.

Suture Method: When splicing is extremely difficult and the boundaries of the magnetic fields are uneven, it'll be better to use the suture method (Ash Johnson, 2000). Before using the suture method, a suture line in the covering area of the two grids must be confirmed (4 options in all, as shown in Fig.8b).

After the way of suture is designated, the cosine function is used to weight the grid. A value within the range from 0 to 1 is confirmed to properly distribute the corrected value between two grids (Fig.9a). To ensure the smoothness of the grid data in the suturing process, a multi-frequency Fourier Transform function is used to search along the suturing line for places where the wavelengths are not matching. The multi-frequency approximation method is used to conduct exterior calibration and the grids are finally spliced together (Fig.9b).

When we think that one grid excels another grid in terms of precision, we can define the grid with higher precision as the reference grid and correct the other grid in complete accordance with the level and trend of the reference grid (WANG Naidong, 2004).

In practice, the blending method is mainly used to splice two grids with similar scales and data qualities and the suture method is mainly used for splicing grids with big differences in magnetic field appearance and grid data quality.

IV. Study on the technology of building high-precision quality control framework grid

4.1 Analysis of the horizontal deviations of long wavelengths in large-area magnetic fields

Considering the unique characteristics of the Aeromagnetic ÄT field and that the magnetic field level of each survey area at their original states is uncertain in the national aeromagnetic map, during the splicing process of grid data between survey areas along the area boundaries, the magnetic field may gradually yield a component of a linear long wavelength. This component, if accumulated, may affect the magnetic field level of the large-area magnetic anomaly (YIN Hang, 2015, WANG Naidong, 2004), triggering the "teeterboard" phenomenon (Fig.10a) and affecting the interpretation of the geotectonic background.

To eliminate the horizontal deviation of the long wavelength of the magnetic field, some scholars have proposed to conduct a 400-km wavelength high pass filtering for the grid with the Cosine roll-off filter. This filter has a smooth shape and its energy spectrum below the cut-off wavelength will not change. To reduce the ringing effect, we

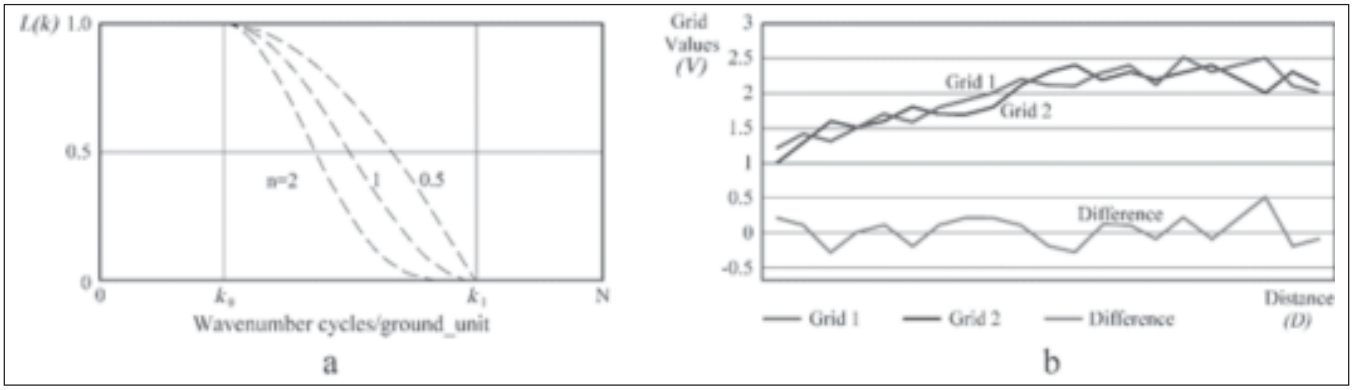

Fig.9 The principle schematic diagram of the suture method (from the Geosoft website) (a) suture weight; (b) multi-frequency suture algorithm

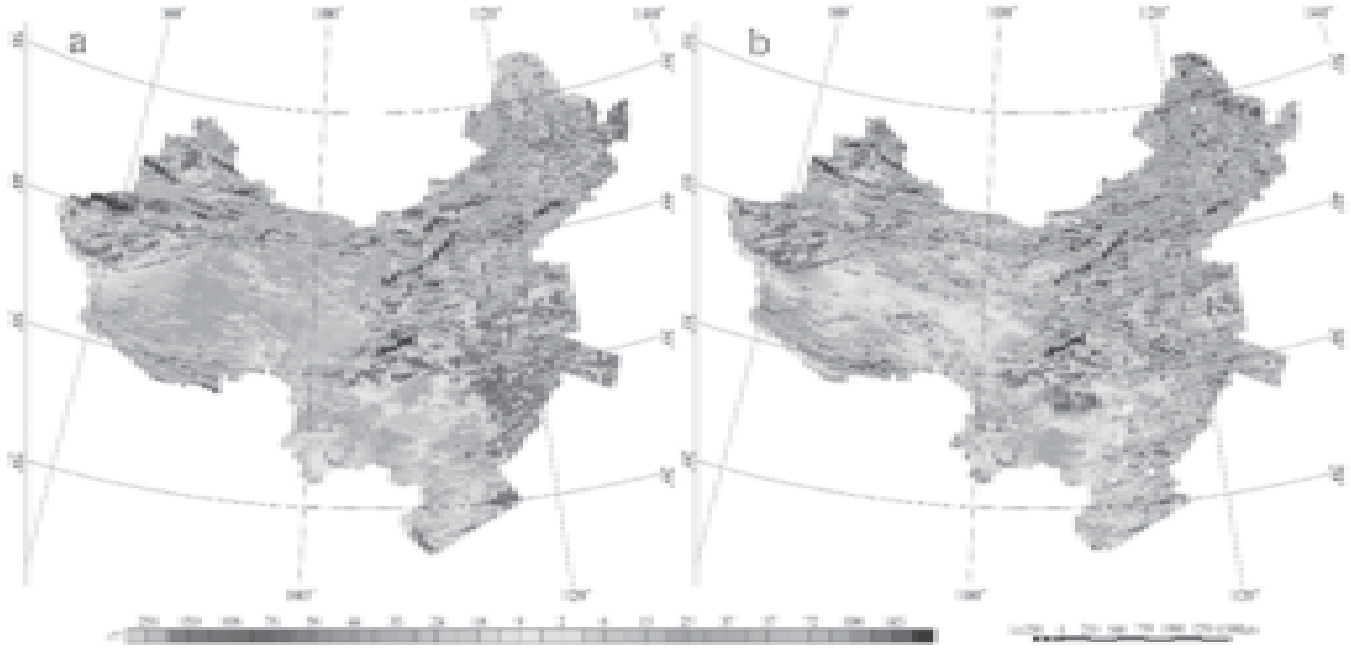

Fig.10 Schematic diagram of the traditional grid splicing method in mapping. (a) result of the traditional grid splicing method; (b) result of the 400-km long wavelength high pass filter magnetic field

have respectively defined the cutoff wavelength and the starting wavelength of the filter as 263 km and 625 km (Cordell, 1985). As can be seen in Fig.10, for the cosine roll-off filter,

,

$$L(k)=\cos^n\left[\frac{\pi}{2}\left(\frac{k-k_0}{k_1-k_0}\right)\right], k_0<k<k_1$$

,

$$L(k)=0, k>k_1,$$

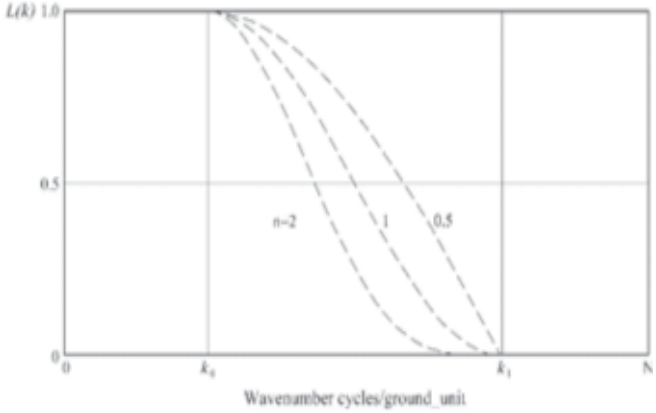

Fig.11 the cosine roll-off filter in long-wavelength filtering (from the Geosoft website)

From Fig 3-5b, it can be seen that after conducting the 400-km wavelength high pass filtering of the aeromagnetic grid data, although the partial magnetic anomaly features become clear, the regional field information with the magnetic field features of the lithosphere as the main part is lost.

4.2 Research on the high-precision control framework grid technology

Theoretically speaking, when compiling large-area aeromagnetic maps, we should build a long on-the-spot survey tie line across the mapping area and build a magnetic control net of the entire mapping area (YIN Hang, 2015) and then splice the aeromagnetic grid data of independent survey areas. By doing so, we can effectively avoid the gradual accumulation of deviations, which may lead to accumulation of horizontal deviations of long wavelength. For example, in the east of the Tibetan Plateau, for the needs of mapping, 4 long tie lines were specially made in the year 2005. With the f long tie lines, through leveling splicing, the stairs trend that appear at the joint boundaries of grids have been effectively improved (Fig.12b) and the effect was better than that with the blending method (as shown in Fig.12a).

Fig.13a shows the national tie line flying work aiming at reducing the long wavelength deviation of MAGDA (P. R. Milligan, R. Franklin. 2004).

However, as of today, there have been no on-the-spot survey tie lines that cross the entire country in China. In order to effectively reduce the accumulation of long wavelength deviation in the splicing process of independent survey areas, in this mapping, we have proposed to use high-precision survey data to build a “high-precision quality control framework grid”, i.e., use the aeromagnetic grid data from independent survey areas with high positioning precision (GPS navigation and positioning) and overlap each other well to build the “framework” and use this framework as the “quality control framework” of the national

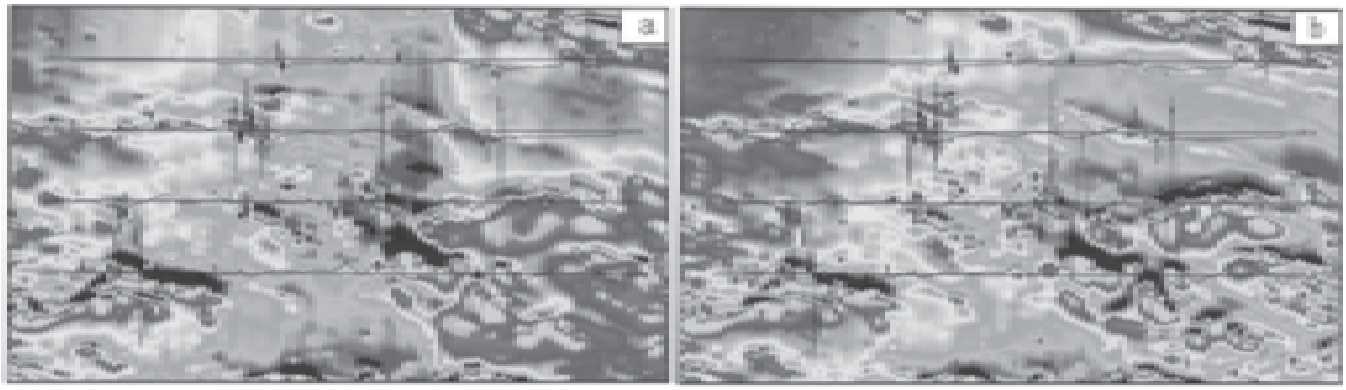

Fig.12 Comparison diagram of the effects of different data splicing methods in the east of the Tibetan Plateau. (a) effect diagram of the blending method; (b) effect diagram of long tie line leveling grid splicing (4 long tie lines are used)

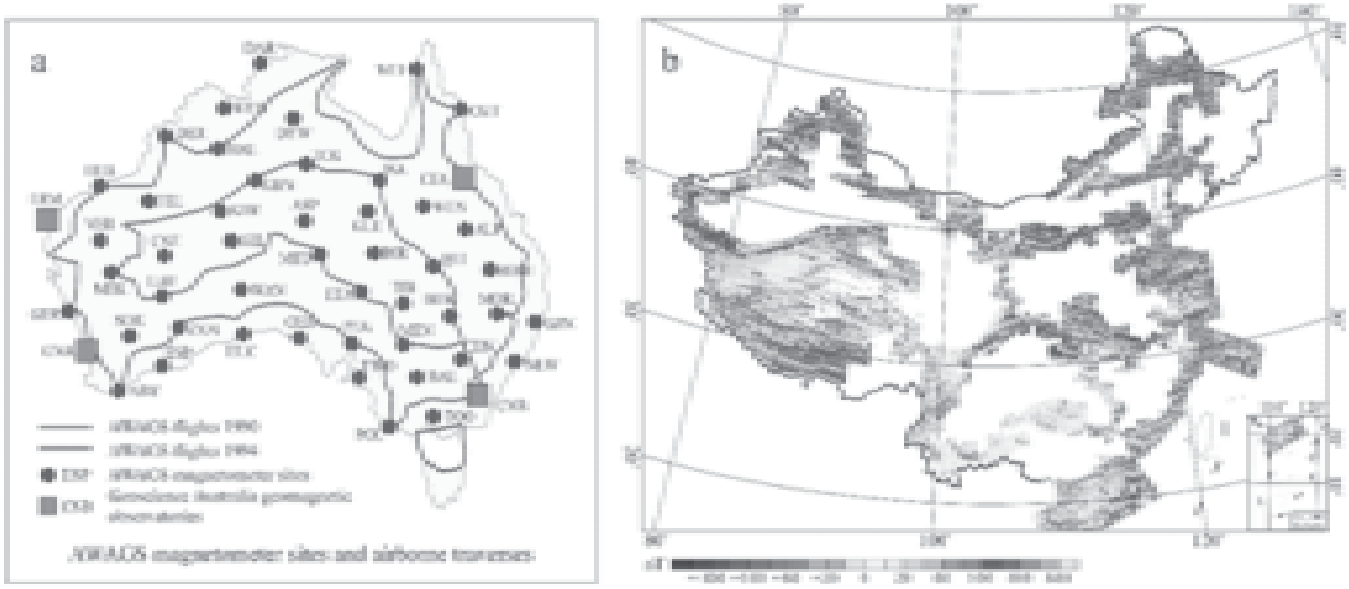

Fig.13 Schematic diagrams of the tie network of Australian and Chinese aeromagnetic mapping. (a) the flying route schematic diagram of the Australian aeromagnetic tie line; (b) the schematic diagram of the "quality control framework grid" in China's aeromagnetic mapping

aeromagnetic mapping. Fig.13b shows a "high-precision quality control framework grid" built by splicing the aeromagnetic grid data of 143 areas surveyed with high precision via the blending or suturing method.

V. Effect analysis on the aeromagnetic mapping of the Chinese land area

Under the calibration of the "high-precision quality control framework grids" and with the "control framework" as the "partial center", the blending and suturing method are respectively used to gradually extend and splice the aeromagnetic grid data of independent survey areas, and finally the national aeromagnetic grid is formed (Fig.14a). This approach has ensured that the deviations in the aeromagnetic grid data from independent survey areas are evenly distributed and has effectively avoided the accumulation of the horizontal deviations of long wavelengths and the "teeter board" phenomenon that is high in the east and low in the west of the magnetic field, thus increasing the reliability of the mapping.

5.1 Effectively retained the magnetic features of the lithosphere

To retain the long wavelength magnetic field of the lithosphere, WDMAM has adopted the method of combining both MAGASAT satellite data (Fig.15b) and the result of 400-km high pass filtering (Fig.14b) (Cohen,Y. 1990, Langel 1998, Maus, 2006);

However, from Fig.14a, it can be seen that although there're some similarities between the results of applying the "high-precision control framework" newly-compiled grid data 400-km low pass filtering and the result of applying the long wavelength satellite (Phillips, J. D.1991, Ravat, D.1995, 2002, Jong Sun Hwang, 2010), there're still some differences in partial magnetic field features. Comparing it with the actual geotectonic background, we find that the partial details of the magnetic map compiled through the "national high-precision

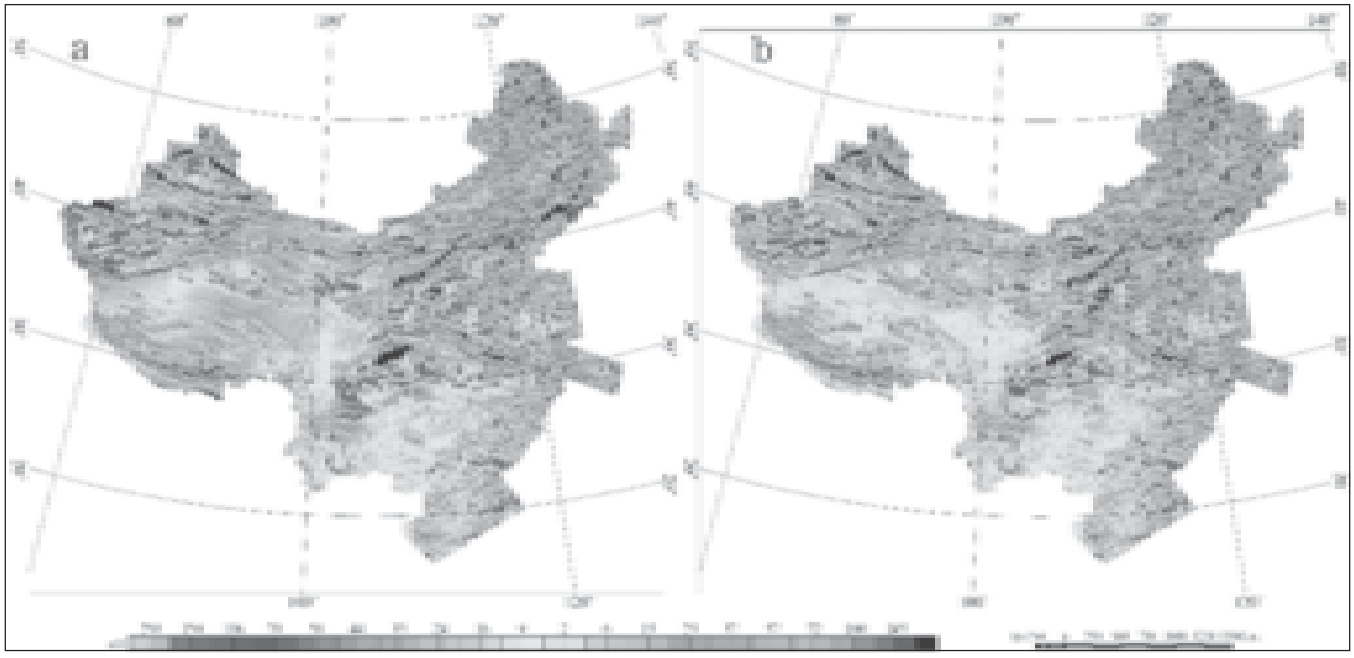

Fig.14 Comparison diagram of the results between the “high precision control framework” mapping and traditional mapping. (a) mapping results obtained via the “high-precision control framework”, (b) mapping results obtained with the “high precision control framework” and 400-km high pass filtering

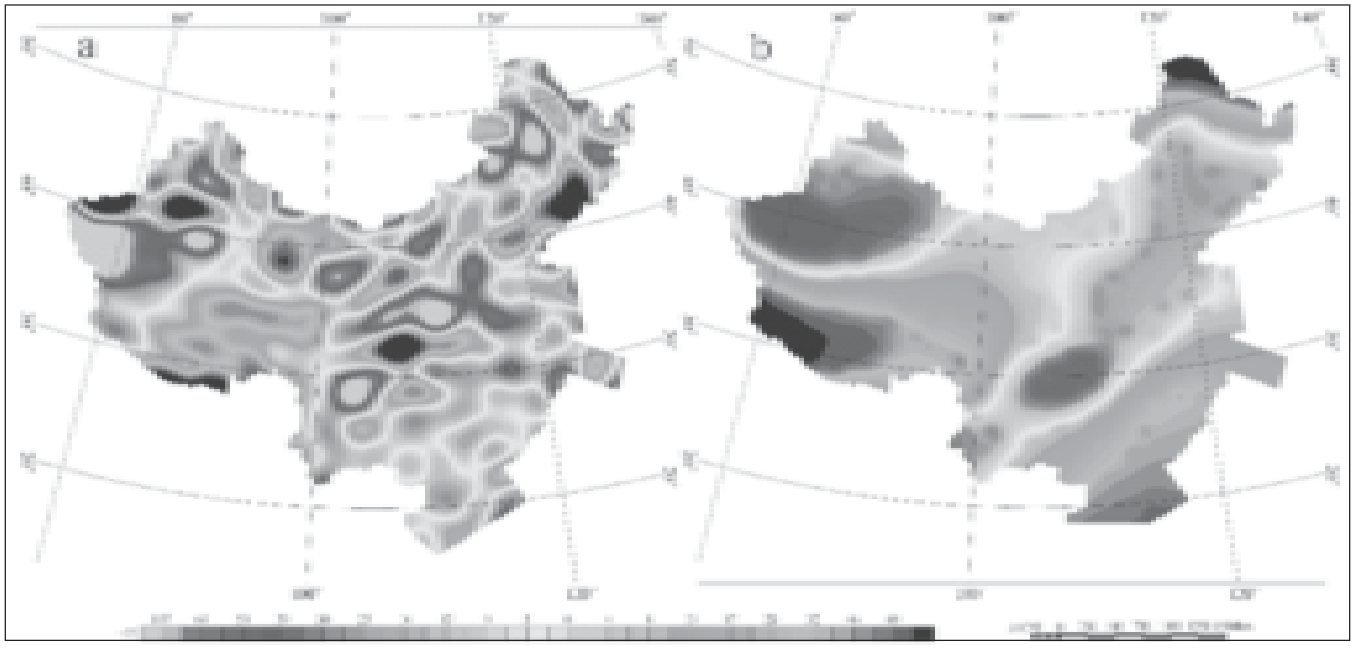

Fig.15 Comparison diagram between the 400 low pass filtering result and the MAGSAT satellite magnetic field result. (a) result obtained with the “high-precision control framework” 400-km low pass filtering; (b) result obtained with the MAGSAT satellite magnetic field

control framework grid” technology is closer to the real geotectonic background (e.g. The background magnetic feature of the Tarim Basin of China) and is therefore of more reference value.

5.2 THE STANDARDIZATION OF SOURCE DATA HAS CORRECTED A LOT OF PROBLEM DATA RECORDS THAT CURBS GEOPHYSICAL UNDERSTANDING

In this mapping process, by standardizing the source data from independent surveying areas, a lot of problem data that curbed the geological understandings in the research on geotectonic background have been corrected. For example, for the area from Nuolgay to Ma’erkang in the northeast of the Tibetan Plateau (Fig.16a), after the original magnetic field data of the area has been standardized, a loose and elevated background anomaly came into being (Fig.16b) and the newly compiled result (Fig.16c,d) suggests that it matches the area from Ganzi to Songpan in the actual geotectonic structure.

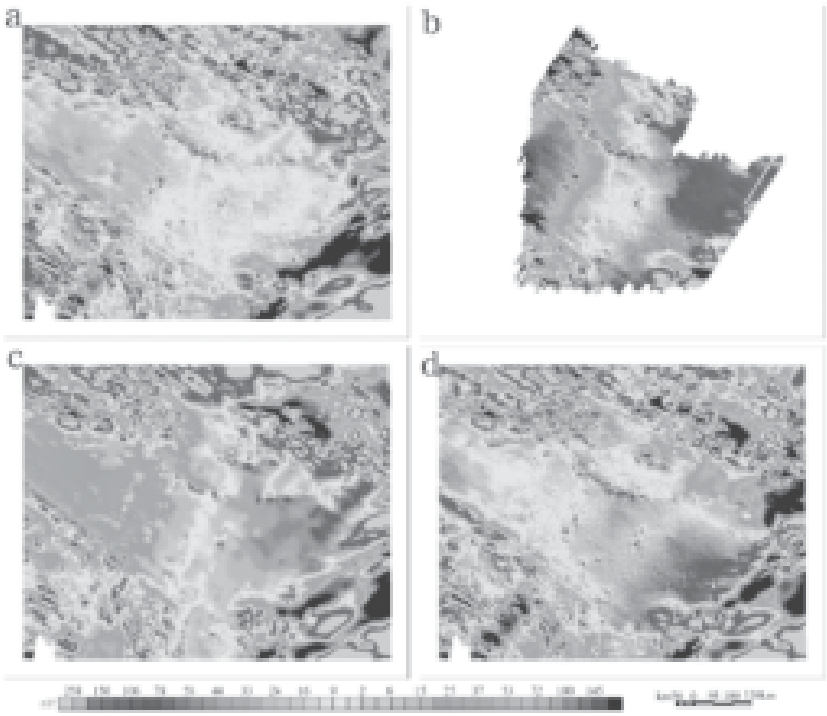

Fig.16 Comparison diagram of the area from Nuolgay to Ma'erkang after the problem data is corrected. (a) old version result of the Chinese magnetic mapping; (b) result of the standardized source data; (c) result obtained with the" high-precision control framework" mapping; (d) result obtained with "high-precision control framework" mapping 400-km high pass filtering

VI. Conclusion

This new aeromagnetic mapping of the Chinese land area has fully borrowed ideas from the experience of the WDMAM project and has conducted five categories of universalized operations for the aeromagnetic materials collected in China over the past 50 years and more. Considering that China is lack of the national data quality tie line, we have proposed to use high-precision survey data to develop a "high-precision quality control framework grid" technology and use this technology to compile the aeromagnetic map of the Chinese land area. This approach has effectively addressed the "teeter board" problem caused by the deviation accumulation of long wavelength and retained the magnetic field features of the lithosphere that may reflect deep-layer geological structures. The outcomes of this research will greatly enhance the application level of the magnetic map of the Chinese land area in geotectonic division and mine resource prospecting.

Reference

[1] S. Maus and T. Sazonova, K. Hemant, et al, (2007): National Geophysical Data Center candidate for the World Digital Magnetic Anomaly Map[J], Geochemistry, Geophysics, Geosystems, 8 (6).

[2] Chiappini, M., A. Meloni, E. Boschi, O. Faggioni, N. Beverini, C. Carmisciano, and I. Marson, (2000): On shore-off shore integrated shaded relief magnetic anomaly map at sea level of Italy and surrounding areas, Ann. Geofis., 43, 983–989.

[3] Socias, I., and J. Mezcua, (1996): Levantamiento aeromagnetico del archipielago canario, Publ. Tec. 35, 28 pp., Inst. Geogr. Nacl., Madrid.

[4] Socias, I., J. Mezcua, J. Lynam, and R. Del Potro, (1991): Interpretation of an aeromagnetic survey of the Spanish mainland, Earth Planet. Sci. Lett., 105 (1–3), 55–64.

[5] Vine, F. J., and D. H. Matthews, (1963): Magnetic anomalies over oceanic ridges, Nature, 199, 947–949.

[6] Cordell L, (1985): Techniques, applications and problems of analytical continuation of New Mexico aeromagnetic data between arbitrary surfaces of very high relief[J], Institut de Geophysique, Universite de Lausanne, Switzerland, Bulletin No.7, 96-99.

[7] Fairhead, J. D., D. J. Misener, C. M. Green, G. Bainbridge, and S. W. Reford, (1997): Large scale compilation of magnetic, gravity and electromagnetic data: The new exploration strategy for the 90's, in Proceedings of Exploration 97: Fourth Decennial International Conference on Mineral Exploration, edited by A. G. Gubins, pp. 805–816, GEO F/X, Toronto, Canada.

[8] Maus, S., H. Lu¨hr, M. Rother, K. Hemant, G. Balasis, P. Ritter, and C. Stolle, (2007): Fifth-generation lithospheric magnetic field model from CHAMP satellite surveys, Geochem. Geophys. Geosyst., 8, Q05013, doi:10.1029/2006GC001521.

[9] Maus, S., M. Rother, R. Holme, H. Lu¨hr, N. Olsen, and V. Haak, (2002): First scalar magnetic anomaly map from CHAMP satellite data indicates weak lithospheric field, Geophys. Res. Lett., 29 (14), 1702, doi:10.1029/2001GL013685.

[10] Wang N D., (2007): Some problems concerning 1, 250000 areomagnetic series maps [J]. Geophysical and Geochemical Exploration (in Chinese), 31 (5) :459?464.

[11] WEN Zhenhe, ZHANG Xunhua, YANG Jinyu, et al. (2011): Digital Compilation of 1:1000 000 Geological and Geophysical Map Series of China and Adjacent Regions on MapGIS Platform [J], Journal of Geo-information Science, 13 (6), 750-757.

[12] Gao Guoming, Kang Guofa, (2010): The Compare Analysis of Satellite Geomagnetic Model Values and

IGRF Model Values with Observed Values of Geomagnetic Observatories in China[J].Journal of Yunnan University, 32 (5): 547-552.

[13] Kang Guofa, Gao Guoming, Bai Chunhua, et al. (2010): Distribution of the Magnetic Anomaly for the CHAMP Satellite in China and Adjacent Areas[J]. Chinese Journal of eophysics, 53 (4) :895-903.

[14] Backus, G. E. (1970): Non-uniqueness of the external geomagnetic field determined by surface intensity surveys, J. Geophys. Res., 75, 6339-6341.

[15] Minty B R S, (1991): Simple micro-levelling for aeromagnetic data[J], Exploration Geophysics, V.22, P591-592.

[16] Naudy H, Dreyer H, (1968): Essai de filtrage non-lineaire applique aux profils aeromagnetiques[J], Geophysical Prospecting, 16 (2), 171-178.

[17] Briggs L C, Machine contouring using minimum curvature[J], Geophysics, 1974, 39 (1), 39-48.

[18] Ash Johnson, Stephen Cheeseman, Julie Ferris, Improved compilation of Antarctic Peninsula magnetic data by new interactive grid suturing and blending methods, 2000.

[19] PGW, GETECH, AGRS, CAG, China Aeromagnetic, Mapping Project (CHAMP), 1996-1999 Technical Report, 1999, V.1, P8-11.

[20] Minty, B. R. S., P. R. Milligan, A. P. J. Luyendyk, and T. Mackey (2003), Merging airborne magnetic surveys into continental-scale compilations, Geophysics, 68, 988–995.

[21] Paterson N, Reford S W, Kwan K CH, (1990): Continuation of magnetic data between arbitrary surfaces:Advances and applications, Society of Exploration Geophysicists Expanded Abstracts, P666-669.

[22] Wang N D. (2004): The Aeromagnetic Anomaly Map of China and the Adjacent Sea Areas (1,5000000) (in Chinese) [M]. Beijing : Geological Publishing House.

[23] YIN Hang, ZHOU Jian-xin, SHU Qing, et al. 2015. The key technologies for making the magnetic anomaly map (1,5,000,000) of China mainland, off shore and adjacent areas. Progress in Geophysics (in Chinese), 30 (5) :2107-2112, doi:10.6038/pg20150514.

[24] Cordell L. (1985): Techniques, applications, and problems of analytical continuation of New Mexico aeromagnetic data between arbitrary surfaces of very high relief [C].//Proceedings of the International Meeting on Potential Fields in Rugged Topography. Institute of Geophysics, University of Lausanne, Switzerland, Bulletin No.7, p.96-99.

[25] P. R. Milligan, R. Franklin, (2004): Abstract A new generation Magnetic Anomaly Grid Database of Australia (MAGDA), Preview 2004 (113) 1-40. Published: Australian Society of Exploration Geophysicists. pp. 25-29.

[26] Cohen, Y., and J. Achache, (1990): New global vector magnetic anomaly maps derived from Magsat data, J. Geophys. Res., 95, 10, 783–10, 800.

[27] Langel, R. A., and W. J. Hinze, (1998): The Magnetic Field of the Earth's Lithosphere: The Satellite Perspective, Cambridge Univ. Press, New York.

[28] Maus, S., H. Lu¨hr, and M. E. Purucker (2006), Simulation of the high-degree lithospheric field recovery for the swarm constellation of satellites, Earth Planets Space, 58, 397-407.

[29] Phillips, J. D., R. L. Reynolds, and H. Frey, (1991): Crustal structure interpreted from magnetic anomalies, Rev. Geophys., 29, 416–427.

[30] Ravat, D., R. A. Langel, M. Purucker, J. Arkani-Hamed, and D. E. Alsdorf, (1995): Global vector and scalar Magsat magnetic anomaly maps, J. Geophys. Res., 100, 20, 111–20, 136.

[31] Ravat, D., K. A. Whaler, M. Pilkington, T. Sabaka, and M. Purucker, (2002): Compatibility of high-altitude aeromagnetic and satellite-altitude magnetic anomalies over Canada, Geophysics, 67, 546-554.

[32] Jong Sun Hwang, Hyung Rae Kim, Mancheol Suh et al.2010. Long-wavelength geopotential fields study of East Asia from satellite data.Chinese Journal Geophysics, 53 (6) : 1327-1335.